

BACE inhibition produces a rapid, non-progressive reduction in volume of amyloid-rich brain regions in patients with Alzheimer's disease

Cyrille Sur, PhD¹, James Kost, PhD¹, David Scott, PhD², Katarzyna Adamczuk, PhD², Nick C. Fox, MD³, Jeffrey L. Cummings, MD, ScD⁴, Pierre N. Tariot, MD⁵, Paul S. Aisen, MD⁶, Bruno Vellas, MD, PhD⁷, Tiffini Voss, MD¹, Erin Mahoney, BA¹, Yuki Mukai, MD¹, Matthew E. Kennedy, PhD¹, Christopher Lines, PhD¹, David Michelson, MD¹ and Michael F. Egan, MD¹

¹Merck & Co., Inc., Kenilworth, NJ, USA

²Bioclinica, Newark, CA, USA

³ Institute of Neurology and UK Dementia Research Institute, University College London, London, UK

⁴University of Nevada Las Vegas (UNLV) School of Integrated Health Sciences; UNLV Department of Brain Health; Chambers-Grundy Center for Transformative Neuroscience; Cleveland Clinic Lou Ruvo Center for Brain Health, Las Vegas, NV, USA

⁵Banner Alzheimer's Institute, University of Arizona College of Medicine, Phoenix, AZ, USA

⁶University of Southern California, San Diego, CA, USA

⁷Gerontopole, INSERM U 1027, Alzheimer's Disease Research and Clinical Center, Toulouse University Hospital, Toulouse, France

Corresponding author: Cyrille Sur, Merck & Co., Inc., West Point, PA, USA. Tel:

+12153530511 email: cyrille.sur@merck.com

Abstract

In the phase-3 EPOCH trial, treatment with the BACE inhibitor verubecestat failed to improve cognition in mild-to-moderate Alzheimer's disease patients but was associated with reduced hippocampal volume after 78 weeks as assessed by magnetic resonance imaging. The aims of the present exploratory analyses were to: 1) further characterise the effect of verubecestat on brain volume by evaluating the time course of volumetric magnetic resonance imaging changes for a variety of brain regions; 2) understand the mechanism through which verubecestat might cause hippocampal (and other brain region) volume loss by assessing its relationship to measures of amyloid, neurodegeneration, and cognition. Participants were aged 55-85 years with probable Alzheimer's disease dementia and a Mini Mental State Examination score ≥ 15 and ≤ 26 . Magnetic resonance images were obtained at baseline and at Weeks 13, 26, 52 and 78 of treatment. Magnetic resonance images were segmented using Freesurfer and analysed using a tensor-based morphometry method. Positron emission tomography amyloid data were obtained with Vizamyil[®] at baseline and Week 78. Standardised uptake value ratios were generated with subcortical white matter as a reference region. Neurofilament light chain in the cerebrospinal fluid was assessed as a biomarker of neurodegeneration. Compared with placebo, verubecestat showed increased magnetic resonance imaging brain volume loss at Week 13 with no evidence of additional loss through Week 78. The verubecestat-related volumetric magnetic resonance imaging loss occurred predominantly in amyloid-rich brain regions. Correlations between amyloid burden at baseline and verubecestat-related volumetric magnetic resonance imaging reductions were not significant ($r = 0.05$ to 0.26 , p values >0.27). There were no significant differences

between verubecestat and placebo in changes from baseline in cerebrospinal fluid levels of neurofilament light chain at Week 78 (increases of 7.2 and 14.6 pg/mL for verubecestat versus 19.7 pg/mL for placebo, p values ≥ 0.1). There was a moderate correlation between volumetric magnetic resonance imaging changes and cognitive decline in all groups including placebo at Week 78 (e.g., $r = -0.45$ to -0.55 , $p < 0.001$ for whole brain), but the correlations were smaller at Week 13 and significant only for the verubecestat groups (e.g., $r = -0.15$ and -0.11 , $p < 0.04$ for whole brain). Our results suggest that the verubecestat-associated magnetic resonance imaging brain volume loss is not due to generalised, progressive neurodegeneration but may be mediated by specific effects on BACE-related amyloid processes. (Clinicaltrials.gov; NCT01739348)

Keywords: BACE, verubecestat, Alzheimer's disease, MRI

Abbreviations:

Alzheimer's Disease Assessment Scale – Cognitive Subscale (11-item version), ADAS-Cog₁₁

β -amyloid precursor protein cleaving enzyme, BACE1

Confidence interval, CI

Glial fibrillary acidic protein, GFAP

Magnetic resonance imaging, MRI

Neurofilament light chain, NfL

Positron emission tomography, PET

Ubiquitin carboxy-terminal hydrolase L1, UCHL1

Volumetric magnetic resonance imaging, vMRI

Short title: BACE inhibition and brain volume in Alzheimer's disease

Accepted Version

Introduction

Inhibition of β -amyloid precursor protein cleaving enzyme (BACE1) has been proposed as a therapeutic strategy to slow Alzheimer's disease progression by reducing β -amyloid production (Yan and Vassar, 2014). Verubecestat is a BACE1 inhibitor that reduces β -amyloid levels by over 60% in the cerebrospinal fluid of patients with Alzheimer's disease (Kennedy *et al.*, 2016). The recent EPOCH trial of verubecestat in patients with mild-to-moderate Alzheimer's disease dementia failed to demonstrate slowing of disease progression over 78 weeks as assessed by measures of cognition and daily function, despite reduction of cerebrospinal fluid β -amyloid and limited but significant reduction of brain amyloid as assessed by amyloid positron emission tomography (PET) (Egan *et al.*, 2018). Verubecestat was also associated with a greater reduction in total hippocampal volume as assessed by magnetic resonance imaging (MRI) compared to placebo at Week 78 (Egan *et al.*, 2018). Similar findings were seen in the APECS trial of verubecestat in prodromal Alzheimer's disease (Egan *et al.*, 2019) and have been reported for some (but not all) other investigational treatments targeting β -amyloid (Fox *et al.*, 2005; Novak *et al.*, 2016), as well as those targeting non-amyloid mechanisms (Fleisher *et al.*, 2011; Turner *et al.*, 2015). Various hypotheses have been proposed to explain the MRI findings including increased neurodegeneration (a negative effect), reduced amyloid and/or inflammation (presumed beneficial effects), or fluid shifts (Fox *et al.*, 2005; Fortea *et al.*, 2014; Novak *et al.*, 2016; Pegueroles *et al.*, 2017) .

In this paper, we report on additional exploratory analyses of volumetric MRI (vMRI) data from EPOCH to provide a more comprehensive assessment of the vMRI loss with verubecestat, including vMRI changes in other brain regions, the time course of

effects, and relation to amyloid. We also examined the possibility that verubecestat might worsen neurodegeneration due to Alzheimer's disease by assessing cerebrospinal fluid measures of neurodegeneration, including neurofilament light (NfL) chain. Finally, we looked at whether there was a relationship between the increased vMRI loss with verubecestat and cognitive decline. Cognitive worsening with verubecestat was observed in the APECS trial in prodromal Alzheimer's disease patients (Egan *et al.*, 2019). There was evidence of an early-onset, but transient, worsening of cognition with verubecestat in the EPOCH trial (Egan *et al.*, 2018).

Our results indicate that the vMRI loss with verubecestat relative to placebo occurred early (by Week 13), did not thereafter increase over time, and was seen predominantly in amyloid-rich brain regions. Cerebrospinal fluid markers of neurodegeneration were not increased with verubecestat. This pattern of results suggests that verubecestat exerts a rapid, sustained, non-progressive, regional effect in amyloid-rich brain regions rather than an ongoing, widespread, acceleration of neurodegeneration. The correlations with the modest cognitive decline at Week 13 were small, suggesting that the vMRI effects may be of limited clinical significance.

Methods

Full details of the trial methods have been previously reported (Egan *et al.*, 2018).

Relevant details are summarised below.

Patients

Eligible patients were aged 55-85 years, had a score of 15-26 on the Mini Mental State Examination (Folstein *et al.*, 1975) and met standard research and clinical criteria for probable Alzheimer's disease dementia (McKhann *et al.*, 1984; American Psychiatric Association, 2000). All patients had an MRI scan or computerised tomography scan if MRI was contraindicated, to exclude alternative causes of dementia. Acetylcholinesterase inhibitors and/or memantine were allowed provided patients were on stable doses prior to screening.

Design and treatment

The trial (MSD Protocol 017; clinicaltrials.gov NCT01739348) enrolled an initial lead-in safety cohort followed by a primary efficacy cohort. The primary efficacy component of the trial consisted of a randomised, double-blind, parallel group, 78-week treatment period with once daily, oral verubecestat 12mg (N=653), 40mg (N=652), or placebo (N=653). Patients who had a new baseline MRI scan performed during the screening period had an end of treatment (planned to be Week 78 for completers) MRI scan. In addition, routine safety MRI scans were initially performed at regular intervals to assess possible amyloid-related imaging abnormalities (Sperling *et al.*, 2012) though these scans

were deemed unnecessary based on Data Monitoring Committee and regulatory feedback and were thus discontinued part-way through the trial.

Biomarker sub-studies were performed to assess: 1) brain amyloid load in patients who underwent PET imaging, and 2) cerebrospinal fluid levels of NfL as a biomarker of neurodegeneration, along with glial fibrillary acidic protein (GFAP), total-tau, and ubiquitin carboxy-terminal hydrolase L1 (UCHL1) as supporting biomarkers of neural injury and astrocyte response (GFAP), in patients who underwent lumbar puncture (Setsuie and Wada, 2007; Ling *et al.*, 2015; Olsson *et al.*, 2016).

The trial was conducted in accordance with principles of Good Clinical Practice and was approved by the relevant institutional review boards. All patients or, where appropriate, their legal representative, provided written informed consent.

Outcome measures

Three-dimensional T1-weighted MRI images were segmented at baseline and follow-up using Freesurfer, a native-space segmentation method (Fischl *et al.*, 2002, 2004), and analysed using a tensor-based morphometry method developed at Bioclinica. Assessment of atrophy using tensor-based morphometry (also known as Jacobian integration) consisted of estimating the volume changes as captured within the deformation fields resulting from applying a symmetric deformable registration technique between a pair of MRI scans (baseline and follow-up), using a non-linear symmetric log-demons deformation technique with robust cross-correlation metric to ensure invertibility of the transformation. The deformation field was then analyzed by computing the determinant

of its Jacobian matrix, which is a measure of local volume change. An integration of the determinant over a region of interest provided an estimation of the change rate of the volume of this brain region over time. vMRI of total brain and hippocampus as well as of a variety of other brain regions were assessed. In addition to vMRI measures, neurodegeneration was also assessed using the Mayo Cortical Thickness Index (Jack *et al.*, 2015).

Brain amyloid load was assessed in a PET subgroup using ¹⁸F-flutemetamol (Vizamyl®) PET imaging at baseline (placebo N=33, 12 mg N=46, 40 mg N=22) and Week 78 (placebo N=14, 12 mg N=19, 40 mg N=9). The standardised uptake value ratio in various brain regions, as detailed in the statistical analysis and results sections herein, was calculated using a subcortical white matter reference region. No partial volume correction was applied.

Cerebrospinal fluid concentrations of NfL, total-tau, GFAP, and UCHL1 were determined in a subgroup of patients with matched baseline and Week 78 cerebrospinal fluid samples (placebo N=37, 12 mg N=31, 40 mg N=50). Measurements were made using the Quanterix Neurology 4-Plex A assay (NfL, total tau, GFAP and UCHL1) and read on a SIMOA HD-1 Analyzer (Quanterix Corporation, Lexington, MA).

Statistical analyses

The population used for the analyses included all available MRI scans from both trial cohorts (the primary phase-3 cohort plus the phase-2 lead-in safety cohort). All analyses were performed on a post-hoc basis and any p-values reported are nominal and not adjusted for multiplicity. All statistical analyses were performed using SAS Versions 9.3

and 9.4 (SAS Institute, Cary, NC, USA). Further details of each analysis are provided in the footnotes of the corresponding results table or figure.

Analyses of regional brain volume changes and time course

The following vMRI brain measures, along with Mayo Cortical Thickness Index, were analysed: total hippocampal volume, left hippocampal volume, right hippocampal volume, whole brain volume, and ventricular volume. Apart from Mayo Cortical Thickness Index, these measures were prespecified for analysis at Week 78 in the primary phase-3 cohort. As a supportive analysis, we also looked at vMRI changes in 31 individual brain regions (detailed in Supplementary Table S2). A longitudinal Analysis of Covariance model was used to analyse change scores, with time treated as a categorical variable. The model adjusted for geographic region, treatment, sex, apolipoprotein E e4 genotype (carrier, noncarrier), baseline use of vitamin E (0-400 International Units /day, > 400 International Units /day), baseline Alzheimer's disease medication (use, no use), trial cohort (safety cohort, main cohort) and the interaction of time-by-treatment, with the baseline values of Mini Mental State Examination and age included as continuous covariates. The baseline value of the dependent variable and the baseline-by-time interaction term were also included. The Week 78 change-from-baseline mean treatment differences (verubecestat – placebo) at each time point, corresponding confidence intervals (CIs), and two-sided p-values were estimated from this model. An unstructured covariance matrix was used to model the correlation among repeated measurements. In the displays of data from these analyses, baseline is plotted at Week -5, which is the mean assessment time of the baseline measurement relative to the first dose of trial medication

at Week 0; this is because MRIs could be performed many weeks before the start of treatment initiation. As a result, there are no data plotted at Week 0. The time course of the verubecestat arms between Week -5 and Week 0 was assumed to follow the same course as the placebo arm. From this Week 0 placebo coordinate, the time course for each respective verubecestat arm was extended to the estimate at the first scheduled postdose timepoint. This graphical approach allows for a more accurate representation of the slope, accounting for the natural progression of Alzheimer's disease. Difference in slope changes from baseline to Week 13, were compared with Week 13 to Week 78 changes, to investigate if there was evidence of an increase in change over time. We also performed subgroup analyses of change in total hippocampal volume, to determine if there were any differential effects based on dementia severity, apolipoprotein E e4 status, age, or sex.

Analyses of the relationship between PET amyloid burden and verubecestat effects on vMRI measures

To determine if the verubecestat treatment effect on vMRI measures differed by level of amyloid burden in different brain regions, we compared the pooled vMRI changes from a sample of amyloid-rich regions to the pooled changes in a sample of amyloid-poor regions for all patients by treatment group. Since amyloid PET ligands have high non-specific binding to white matter, the PET standardised uptake value ratio can be high in amyloid-poor regions of white matter. Hence, the designation of a brain region as “amyloid-rich” versus “amyloid-poor” was based on previous reports in the literature and confirmed in the PET subgroup included in the trial. Amyloid-rich regions were: pericalcarine cortex, insula cortex, precentral cortex, amygdala, isthmus cingulate cortex,

precuneus cortex, postcentral cortex, lateral occipital cortex, supramarginal cortex, cuneus cortex, lateral orbitofrontal cortex, posterior cingulate cortex, parahippocampal cortex, lingual cortex, paracentral cortex, thalamus, medial orbitofrontal cortex, fusiform cortex, frontal pole cortex, middle temporal cortex, and entorhinal cortex. Amyloid-poor regions were: cerebellum (cortex and white matter), corpus callosum (mid anterior, posterior, central, mid posterior, anterior), and pallidum. As a supportive analysis we also assessed verubecestat effects using an “early amyloid deposition” versus “late amyloid deposition” versus “no amyloid” classification scheme (Mattson *et al.* 2019). “Early amyloid deposition” regions were precuneus, posterior cingulate, isthmus cingulate, insula, and medial and lateral orbitofrontal cortices; “late amyloid deposition” regions were lingual, pericalcarine, paracentral, precentral, and postcentral cortices; and “no amyloid” regions were cerebellar cortex and pallidum. Second, we looked at the correlation between baseline PET amyloid standardised uptake value ratio in a range of amyloid-rich brain regions, selected to cover the full range of standardised uptake value ratio baseline values (detailed in Figure 3), and the verubecestat-placebo difference in vMRI changes for those regions at Week 13 and Week 78; this analysis was performed using simple linear regression. Finally, to test the hypothesis that the decrease in vMRI parameters is due to the loss of amyloid plaque, we looked at the relationship between the percentage change from baseline in PET amyloid standardised uptake value ratio at Week 78 and the percentage change from baseline in hippocampal vMRI at Week 78 for patients in the PET subgroup (a Week 13 analysis could not be performed because PET scans were not conducted at Week 13).

Analyses of the relationship between verubecestat vMRI effects and measures of Alzheimer's disease -related neurodegeneration

Two analyses were performed. First, we assessed the change from baseline in cerebrospinal fluid NfL, and other biomarkers of neurodegeneration (total tau and UCHL1) and gliosis (GFAP) in the cerebrospinal fluid subgroup, to see if there was an increase in the verubecestat groups over time and relative to placebo. Second, we examined whether verubecestat treatment accelerated vMRI changes due to Alzheimer's disease. To do so, the degree of Alzheimer's disease -related neurodegeneration in the placebo group (change in vMRI from baseline at Week 78) was estimated in 31 brain regions (detailed in Supplementary Figure S2). We then investigated correlations between the regional change in the placebo group (i.e., the amount of disease-related neurodegeneration at Week 78) and the regional verubecestat-placebo difference at Week 13 and Week 78. Regional values were derived from the averages of patients within each group. If verubecestat was increasing Alzheimer's disease -related neurodegeneration, then it might show a greater effect in regions with greater disease-related neurodegeneration.

Analysis of the relationship between verubecestat vMRI effects and cognition

Linear regressions of change from baseline for the 11-item Alzheimer's Disease Assessment Scale – Cognitive Subscale (ADAS-Cog₁₁) total score (a standard measure of cognition; Rosen et al. 1984) on change from baseline for the following vMRI parameters at Week 13 and Week 78 were conducted: total hippocampal volume, left hippocampal

volume, right hippocampal volume, whole brain volume, ventricular volume, and Mayo Cortical Thickness Index.

Data availability

MSD's data sharing policy, including restrictions, is available at http://engagezone.msd.com/ds_documentation.php. Requests for access to the clinical trial data can be submitted through the EngageZone site or via email to dataaccess@merck.com.

Results

Patient characteristics

The characteristics of patients who had an MRI were similar across treatment groups (Table 1).

Time course of verubecestat effects on MRI brain measures

In all trial groups, including placebo, brain vMRI measures/Mayo Cortical Thickness Index other than ventricular volume decreased over time (Figure 1, Table 2). Conversely, as expected, ventricular volume increased over time. These changes in brain vMRI measures and Mayo Cortical Thickness Index were more marked in the verubecestat groups versus placebo and were apparent at the earliest imaging time point (Week 13). The verubecestat-related difference from placebo did not increase further at later time

points (Figure 1), as shown by the lack of change in the slope of the verubecestat-placebo treatment difference between Week 13 and Week 78 (Table 3). This pattern of findings was consistent across subgroups defined by age, sex, baseline Mini Mental State Examination severity and apolipoprotein E e4 genotype (Supplementary Table S1).

Results for additional individual brain regions are shown in Supplementary Table S2. The largest volume loss at Week 78 in the placebo arm was observed in entorhinal cortex (-6.5%), amygdala (-5.4%), fusiform cortex (-5.5%) and precuneus cortex (-4.7%). This is consistent with the total hippocampal volume loss of 5% in the placebo group (Table 2) and the fact that these regions are among the first to show accumulation of neurofibrillary tangles and subsequent neurodegeneration.

Relationship between PET amyloid burden and verubecestat effects on vMRI measures

We explored the relationship between PET and vMRI effects in three separate analyses. First, the pattern of verubecestat effects on vMRI reduction in amyloid-rich versus amyloid-poor brain regions over time is shown in Figure 2. The verubecestat-related vMRI loss at Week 13 was predominantly in the amyloid-rich regions, while there were no significant treatment effects in amyloid-poor regions (i.e. white matter regions, cerebellum, pallidum) (Supplementary Table S3). Results for individual brain regions (as opposed to pooling of regions as “amyloid-rich” or “amyloid-poor”) are shown in Supplementary Table S2. The verubecestat-related vMRI loss at Week 13 was most prominent in cuneus cortex, fusiform cortex, insula cortex, lateral occipital cortex,

precuneus cortex, and supramarginal cortex, regions that are implicated in the early stage of Alzheimer's disease and with significant amyloid deposition. On the other hand, no significant treatment effect was observed at Week 13 in white matter regions (e.g. corpus callosum, cerebellum white matter) and gray matter structures (e.g. caudate, cerebellum cortex) with very low to no amyloid deposition in the early stage of the disease. In the analysis using the Mattson classification of brain regions based on timing of amyloid deposition, the verubecestat-related vMRI loss at Week 13 was predominantly in the "early amyloid deposition" and "late amyloid deposition" regions, with no significant treatment effects in the "no amyloid" regions (Supplementary Figure S1 and Supplementary Table S3). The effects of verubecestat did not appear to differ between the "early amyloid deposition" and "late amyloid deposition" regions.

Second, we examined the correlation between baseline PET amyloid SUVR and verubecestat-placebo difference in vMRI changes at Week 13 and Week 78 in 20 amyloid-rich brain regions. The results indicate that the verubecestat effect on vMRI reduction was not significantly correlated with the amount of regional amyloid at baseline (Figure 3) in amyloid-rich brain regions.

Third, to explore whether the reduced vMRI measures were related to the amount of reduction of amyloid, we investigated the relationship between the percentage change from baseline in PET amyloid standardised uptake value ratio at Week 78 and the percentage change from baseline in total hippocampal vMRI at Week 78 in the PET subgroup (placebo N=14, 12mg N=19, 40mg N=9). Directionally, the slopes for verubecestat suggested that patients with less reduction in PET amyloid standardised uptake value ratio had relatively greater hippocampal vMRI loss (Figure 4). Thus, the

inverse relationship does not support the hypothesis that the amount of reduction of amyloid is the reason for the reduced vMRI measures.

Analyses exploring whether verubecestat might increase neurodegeneration

We explored the relationship between vMRI changes and neurodegeneration in two analyses. First, we assessed markers of neurodegeneration in the cerebrospinal fluid of patients in the cerebrospinal fluid subgroup (placebo N=37, 12 mg N=31, 40mg N=50). No significant differences between verubecestat and placebo changes from baseline were seen for cerebrospinal fluid NfL or other biomarkers (Table 4). Second, we examined the correlation between the Week 78 change from baseline in vMRI in the placebo group (i.e., the amount of Alzheimer's disease-related neurodegeneration) and the verubecestat-placebo difference at Week 13 and Week 78 in 31 brain regions. The correlations were generally small and not significant, suggesting that verubecestat did not accelerate the brain loss attributable to Alzheimer's disease (Supplementary Figure S2).

Relationship between verubecestat-related vMRI brain changes and cognition

vMRI changes at Week 13 across the brain regions analysed showed no consistent relationship with change from baseline in ADAS-Cog₁₁ total score at Week 13 (Supplementary Table S3). Based on the small correlation coefficients ($r \leq 0.15$), changes in vMRI measures appear to account for less than 3% of the observed changes in cognition and the findings did not suggest a relationship with dose. At Week 78, findings were similar for the correlation between hippocampal volume and ADAS-Cog₁₁ total score ($r \leq 0.10$) but there appeared to be a moderate relationship between other vMRI

measures (whole brain volume, ventricular volume, Mayo Cortical Thickness Index) and ADAS-Cog₁₁ total score ($r = 0.44$ to 0.55) that was similar between placebo and verubecestat groups.

Discussion

In the EPOCH trial of patients with mild-to-moderate Alzheimer's disease dementia, we found that MRI brain volume decreased over 78 weeks in all trial groups, as expected in a neurodegenerative disorder and reported in previous clinical trials (Novak *et al.*, 2016). However, brain vMRI loss was greater in the verubecestat group than the placebo group. The verubecestat-associated brain vMRI loss occurred early, by the first assessment at Week 13, and did not progress further thereafter relative to placebo.

The mechanisms involved in the early verubecestat-specific brain volume loss are not clear. Several observations suggest that the effect is not due to a progressive neurodegenerative or neurotoxic process. First, there was no significant difference between verubecestat and placebo in cerebrospinal fluid NfL concentrations, a putative marker of neurodegeneration (Olsson *et al.*, 2016) at Week 78. Second, the verubecestat-related vMRI effects did not progress further relative to placebo after Week 13, as might be expected for a chronic neurodegenerative process or a continuing drug-related toxic effect. Third, the verubecestat-related vMRI changes were not occurring in areas of active Alzheimer's disease-related degeneration. While an acute neurodegenerative insult cannot be excluded, taken together, these results suggest some other process may account for the volumetric effects and that this effect was non-progressive.

An important finding from our analyses was that the increased vMRI loss associated with verubecestat appeared to occur predominantly in amyloid-rich brain

areas. The verubecestat-associated loss was similar in brain regions that typically show amyloid deposition earlier versus later in the disease process. Because verubecestat reduces brain amyloid, one might hypothesise that the verubecestat-related vMRI reduction in amyloid-rich regions reflects removal of amyloid. However, several observations suggest that this cannot explain the volume changes seen. First, the magnitude of the amyloid reduction is not likely to be large enough to explain the vMRI reduction. Results from the PET substudy suggest that verubecestat reduced amyloid load by less than 1% at Week 13, a reduction that was too small to explain the approximately 1% reduction in total brain volume at Week 13. Second, the verubecestat effect on regional vMRI reduction was not correlated with the regional amyloid load at baseline. Third, the verubecestat-related change from baseline in amyloid load at Week 78 within patients was not positively correlated with the verubecestat-related change from baseline in hippocampal vMRI at Week 78 (the findings suggested the opposite relationship - greater hippocampal vMRI loss with less reduction in amyloid load).

An alternative explanation is that changes in the amyloid plaque microenvironment could account for the vMRI changes. BACE1 inhibition in plaque microdomains might, for example, change the extent of neuritic dystrophy and/or the inflammatory processes, which could lead to fluid/cellular organization shifts that are detectable by MRI. This hypothesis is indirectly supported by known BACE1-induced enrichment (2-4 fold) in the abundant dystrophic neurites surrounding the amyloid plaque (Zhao *et al.*, 2007). On the other hand, vMRI loss has been reported for non-BACE1 and non-amyloid treatments raising the possibility that the underlying mechanisms could be

multifactorial (Fox *et al.*, 2005; Fleisher *et al.*, 2011; Turner *et al.*, 2015; Novak *et al.*, 2016).

We evaluated whether the early verubecestat-specific MRI brain volume loss was associated with clinical effects. As noted in the Introduction, there was some evidence of an early-onset (Week 13) worsening of cognition with verubecestat relative to placebo in the EPOCH trial but there was no treatment difference at Week 78 (Egan *et al.*, 2018). The correlations between vMRI changes and ADAS-Cog₁₁ total score at Week 13 were generally weak and of modest nominal significance. In contrast, the correlations at Week 78 were much more robust and similar between placebo and verubecestat groups, likely due to ongoing Alzheimer's disease -related neurodegeneration. Overall, verubecestat-specific vMRI loss may be related to some cognitive worsening, but the data presented here suggests the impact is small in this patient population. Other trials reporting a treatment-related vMRI loss in patients with Alzheimer's disease have found worsening in cognition relative to placebo, no change in cognition relative to placebo, or reported conflicting results depending on the assessment instrument (Fox *et al.*, 2005; Fleisher *et al.*, 2011; Turner *et al.*, 2015; Novak *et al.*, 2016; Egan *et al.*, 2019). Given that large numbers of comparisons are typically performed for multiple cognitive endpoints in clinical trials, it is possible that isolated findings are a chance occurrence.

In summary, we performed the most detailed analysis to date on the relationship of anti-amyloid therapy to MRI brain volume loss, a relationship previously observed with several anti-amyloid therapies acting via a variety of mechanisms. Verubecestat was associated with brain vMRI loss that occurred early and did not progress in brain regions with amyloid pathology. Our results suggest that verubecestat was not associated with a

generalised progressive neurotoxic effect but may have exerted specific and relatively rapid effects via amyloid-related processes. The underlying mechanism of the effect is unknown; we speculate that it could be due to effects on inflammation or fluid shifts in the amyloid microenvironment. The clinical relevance of the effect appears to be limited. Caution should be exercised in interpreting these analyses due to their exploratory and *post hoc* nature, no adjustment for multiplicity, and limited sample sizes in some cases (e.g., correlation analyses involving PET amyloid standardised uptake value ratio, analysis of cerebrospinal fluid biomarkers). Key questions for future studies include determining the timing of onset of effect, whether the effect persists after treatment discontinuation, and the underlying mechanism(s) involved.

Funding

This study was funded by Merck Sharp & Dohme Corp., a subsidiary of Merck & Co., Inc., Kenilworth, NJ, USA (MSD).

Competing Interests

CS, JK, TV, EM, YM, MK, CL, DM, and MFE are current or former employees of Merck Sharp & Dohme Corp., a subsidiary of Merck & Co., Inc., Kenilworth, NJ, USA (MSD), and own or owned stock options in Merck & Co., Inc., Kenilworth, NJ, USA.

DS and KA worked as contractors to MSD for the imaging analyses.

NCF has received fees (paid to University College London) for consultancy from Janssen, Eli Lilly, Novartis, Sanofi, Roche, and GlaxoSmithKline and for serving on a data monitoring committee for Biogen. He acknowledges support from the NIHR UCL/H Biomedical Research Centre and the UK Dementia Research Institute.

JLC has provided consultation to Acadia, Actinogen, Alkahest, Allergan, Alzheon, Annovis, Avanir, Axsome, BiOasis, Biogen, Bracket, Cassava, Cerecin, Cortexyme, Diadem, EIP Pharma, Eisai, Foresight, GemVax, Genentech, Green Valley, Grifols, Hisun, Merck, Otsuka, Resverlogix, Roche, Samumed, Samus, Takeda, Third Rock and United Neuroscience pharmaceutical and assessment companies. He has stock options in Prana, Neurokos, ADAMAS, MedAvante, QR pharma, BiOasis. He is supported by KMA; NIGMS grant P20GM109025; NINDS grant U01NS093334; and NIA grant R01AG053798PNT has received consulting fees from Acadia, AbbVie, AC Immune,

Auspex, Boehringer-Ingelheim, Chase Pharmaceuticals, Eisai, GliaCure, Insys Therapeutics, Pfizer. He has received consulting fees and research support from AstraZeneca, Avanir, Eli Lilly, Lundbeck, MSD, Roche, and research support only Amgen, Avid, Biogen, Elan, Functional Neuromodulation (f(nm)), GE Healthcare, Genentech, Novartis, and Targacept. He has received other research support from the NIA and Arizona Department of Health Services and holds stock options in ADAMAS.

PSA has served as a consultant to the following companies: NeuroPhage, Eli Lilly, MSD, Avanir, Roche, Novartis, Pfizer, AstraZeneca, Janssen, Lundbeck, Biogen, Probiodrug, Anavex, Abbvie, Janssen, Cytos, aTyr. He receives research support from Eli Lilly, Janssen, the Alzheimer's Association and the NIH.

BV has served as a consultant to the following companies: Transition Therapeutics, Takeda, Otsuka, Lilly, Nestlé, MSD, Biogen, Roche. He receives research support from: Abbvie, Lilly, MSD, Otsuka, Sanofi, Alzheon, Astra-Zéneca, LPG Systems Nestlé, The Alzheimer's Association, The Alzheimer Drug Discovery Foundation, The European Commission and French Ministry of Health.

Acknowledgments

We thank the patients, caregivers, families, and site investigators and their staff who participated in the trial.

References

American Psychiatric Association. Diagnostic and Statistical Manual of Mental Disorders. 4th edition; 2000. Arlington, VA.

Egan MF, Kost J, Tariot PN, Aisen PS, Cummings JL, Vellas B, *et al.* Randomized Trial of Verubecestat for Mild-to-Moderate Alzheimer's Disease. *N Engl J Med* 2018; 378(18): 1691-703.

Egan MF, Kost J, Voss T, Mukai Y, Aisen PS, Cummings JL, *et al.* Randomized Trial of Verubecestat for Prodromal Alzheimer's Disease. *N Engl J Med* 2019; 380(15): 1408-20.

Fischl B, Salat DH, Busa E, Albert M, Dieterich M, Haselgrove C, *et al.* Whole Brain Segmentation: Automated Labeling of Neuroanatomical Structures in the Human Brain. *Neuron* 2002;33:341-355.

Fischl B, van der Kouwe A, Destrieux C, Halgren E, Segonne F, Salat D, *et al.* Automatically Parcellating the Human Cerebral Cortex. *Cerebral Cortex* 2004;14:11-22.)

Fleisher AS, Truran D, Mai JT, Langbaum JB, Aisen PS, Cummings JL, *et al.* Chronic divalproex sodium use and brain atrophy in Alzheimer disease. *Neurology* 2011; 77(13): 1263-71.

Folstein MF, Folstein SE, McHugh PR. "Mini-mental state". A practical method for grading the cognitive state of patients for the clinician. *J Psychiatr Res* 1975; 12(3): 189-98.

Fortea J, Vilaplana E, Alcolea D, Carmona-Iragui M, Sánchez-Saudinos MB, Sala I, *et al.* Cerebrospinal fluid β -amyloid and phospho-tau biomarker interactions affecting brain structure in preclinical Alzheimer disease. *Ann Neurol.* 2014;76(2):223-30.

Fox NC, Black RS, Gilman S, Rossor MN, Griffith SG, Jenkins L, *et al.* Effects of Abeta immunization (AN1792) on MRI measures of cerebral volume in Alzheimer disease. *Neurology* 2005; 64(9): 1563-72.

Jack CR, Jr., Wiste HJ, Weigand SD, Knopman DS, Mielke MM, Vemuri P, *et al.*
Different definitions of neurodegeneration produce similar amyloid/neurodegeneration
biomarker group findings. *Brain* 2015; 138(Pt 12): 3747-59.

Kennedy ME, Stamford AW, Chen X, Cox K, Cumming JN, Dockendorf MF, *et al.* The
BACE1 inhibitor verubecestat (MK-8931) reduces CNS beta-amyloid in animal models
and in Alzheimer's disease patients. *Sci Transl Med* 2016; 8(363): 363ra150.

Ling H, Hardy J, Zetterberg H. Neurological consequences of traumatic brain injuries in
sports. *Mol Cell Neurosci* 2015; 66(Pt B): 114-22.

Mattsson N, Palmqvist S, Stomrud E, Vogel J, Hansson O. Staging β -amyloid
pathology with amyloid positron emission tomography. *JAMA Neurol.* 2019 Jul 17.
doi: 10.1001/jamaneurol.2019.2214. [Epub ahead of print]

McKhann G, Drachman D, Folstein M, Katzman R, Price D, Stadlan EM. Clinical
diagnosis of Alzheimer's disease: report of the NINCDS-ADRDA Work Group under the
auspices of Department of Health and Human Services Task Force on Alzheimer's
Disease. *Neurology* 1984; 34(7): 939-44.

Novak G, Fox N, Clegg S, Nielsen C, Einstein S, Lu Y, *et al.* Changes in Brain Volume
with Bapineuzumab in Mild to Moderate Alzheimer's Disease. *J Alzheimers Dis* 2016;
49(4): 1123-34.

Olsson B, Lautner R, Andreasson U, Ohrfelt A, Portelius E, Bjerke M, *et al.* SUVR and
blood biomarkers for the diagnosis of Alzheimer's disease: a systematic review and meta-
analysis. *Lancet Neurol* 2016; 15(7): 673-84.

Pegueroles J, Vilaplana E, Montal V, Sampedro F, Alcolea D, Carmona-Iragui M,

et al. Longitudinal brain structural changes in preclinical Alzheimer's disease. *Alzheimers Dement.* 201;13(5):499-509.

Rosen WG, Mohs RC, Davis KL. A new rating scale for Alzheimer's disease. *Am J Psychiatry* 1984;141:1356-64.

Setsuie R, Wada K. The functions of UCH-L1 and its relation to neurodegenerative diseases. *Neurochem Int* 2007; 51(2-4): 105-11.

Sperling R, Salloway S, Brooks DJ, Tampieri D, Barakos J, Fox NC, *et al.* Amyloid-related imaging abnormalities in patients with Alzheimer's disease treated with bapineuzumab: a retrospective analysis. *Lancet Neurol* 2012; 11(3): 241-9.

Turner RS, Thomas RG, Craft S, van Dyck CH, Mintzer J, Reynolds BA, *et al.* A randomized, double-blind, placebo-controlled trial of resveratrol for Alzheimer disease. *Neurology* 2015; 85(16): 1383-91.

Yan R, Vassar R. Targeting the beta secretase BACE1 for Alzheimer's disease therapy. *Lancet Neurol* 2014; 13(3): 319-29.

Zhao J, Fu Y, Yasvoina M, Shao P, Hitt B, O'Connor T, *et al.* Beta-site amyloid precursor protein cleaving enzyme 1 levels become elevated in neurons around amyloid plaques: implications for Alzheimer's disease pathogenesis. *J Neurosci* 2007; 27(14): 3639-49.

Table 1: Baseline characteristics of patients

	Verubecestat 12mg (N=464 ^a)	Verubecestat 40mg (N=455 ^a)	Placebo (N=477 ^a)
Demographics			
Age - years, mean (SD)	70.7 (7.4)	71.4 (7.4)	71.9 (7.6)
Female, n (%)	253 (54.5)	268 (58.9)	256 (53.7)
Apolipoprotein E ε4 carrier, n (%)	301 (64.9)	277 (60.9)	323 (67.7)
Mild severity (Mini Mental State Examination score ≥21), n (%)	228 (49.1)	217 (47.7)	227 (47.6)
Alzheimer's disease treatment, n (%)	411 (88.6)	406 (89.2)	430 (90.1)
Education <undergraduate degree, n (%)	284 (61.2)	260 (57.1)	280 (58.7)
Mean (SD) baseline vMRI values			
Whole brain volume, mL	973 (105)	961 (104)	966 (98)
Total hippocampal volume, μL	5852 (1202)	5801 (1170)	5791 (1046)
Left hippocampal volume, μL	2879 (618)	2839 (592)	2839 (541)
Right hippocampal volume, μL	2973 (629)	2963 (615)	2953 (552)
Ventricular volume, mL	49 (22)	49 (21)	51 (22)
Mayo cortical thickness index, mm	2.5 (0.2)	2.5 (0.2)	2.5 (0.2)
Biomarker Alzheimer's disease diagnosis in PET amyloid sub-study^b			
Alzheimer's disease positive, n/N (%)	43/46 (93.5)	21/22 (95.5)	29/33 (87.9)

^aN is the number of patients in the full-analysis-set for total hippocampal volume (the prespecified key MRI endpoint in the original report (Egan *et al.*, 2018))

^bPositivity based on visual read of ¹⁸F-flutemetamol PET scans according to the product label; N is the number of patients who had a baseline MRI and a baseline PET scan

Table 2: Percent change in MRI brain volume measures from baseline to Week 13 and Week 78, model-based least-squares mean (95% CI) and difference (95% CI) versus placebo

MRI Measure	Timepoint ^a	Mean Change from Baseline ^a (95% CI)			Difference vs Placebo (95% CI)			
		Verubecestat 12mg	Verubecestat 40mg	Placebo	12mg vs placebo	p Value	40mg vs placebo	p Value
Total hippocampal volume	Week 13	-1.9 (-2.0, -1.7)	-1.8 (-2.0, -1.7)	-1.2 (-1.3, -1.0)	-0.7 (-0.9, -0.5)	<0.001	-0.6 (-0.8, -0.4)	<0.001
	Week 78	-5.6 (-5.8, -5.3)	-5.6 (-5.8, -5.4)	-5.0 (-5.2, -4.7)	-0.6 (-0.9, -0.3)	<0.001	-0.6 (-1.0, -0.3)	<0.001
Left hippocampal volume	Week 13	-1.9 (-2.1, -1.7)	-1.8 (-2.0, -1.6)	-1.2 (-1.4, -1.1)	-0.6 (-0.9, -0.4)	<0.001	-0.5 (-0.8, -0.3)	<0.001
	Week 78	-5.6 (-5.9, -5.4)	-5.6 (-5.9, -5.3)	-5.0 (-5.2, -4.7)	-0.7 (-1.1, -0.3)	<0.001	-0.7 (-1.0, -0.3)	<0.001
Right hippocampal volume	Week 13	-1.9 (-2.1, -1.7)	-1.9 (-2.0, -1.7)	-1.1 (-1.3, -1.0)	-0.7 (-1.0, -0.5)	<0.001	-0.7 (-0.9, -0.5)	<0.001
	Week 78	-5.5 (-5.7, -5.2)	-5.6 (-5.8, -5.3)	-5.0 (-5.2, -4.7)	-0.5 (-0.9, -0.2)	0.004	-0.6 (-1.0, -0.2)	0.001
Whole brain volume	Week 13	-1.0 (-1.0, -0.9)	-1.0 (-1.1, -0.9)	-0.6 (-0.6, -0.5)	-0.4 (-0.5, -0.3)	<0.001	-0.4 (-0.5, -0.3)	<0.001
	Week 78	-2.9 (-3.1, -2.8)	-2.9 (-3.1, -2.8)	-2.5 (-2.6, -2.4)	-0.4 (-0.6, -0.3)	<0.001	-0.5 (-0.6, -0.3)	<0.001
Ventricular volume	Week 13	4.1 (3.7, 4.4)	4.2 (3.9, 4.5)	2.9 (2.6, 3.2)	1.1 (0.7, 1.5)	<0.001	1.2 (0.8, 1.7)	<0.001
	Week 78	16.1 (15.3, 17.0)	16.1 (15.3, 17.0)	15.8 (15.0, 16.6)	0.3 (-0.8, 1.5)	0.594	0.8 (-0.3, 2.0)	0.168
Mayo Cortical Thickness Index	Week 13	-1.9 (-2.0, -1.7)	-1.8 (-1.9, -1.6)	-1.3 (-1.4, -1.1)	-0.6 (-0.7, -0.4)	<0.001	-0.5 (-0.7, -0.3)	<0.001
	Week 78	-6.1 (-6.4, -5.8)	-5.8 (-6.2, -5.5)	-5.4 (-5.7, -5.1)	-0.7 (-1.1, -0.3)	<0.001	-0.4 (-0.8, -0.1)	0.022

^a Note: baseline MRI was performed a mean of -5 weeks prior to the initiation of treatment. The timepoints shown (Week 13 and Week 78) are relative to the initiation of treatment, not relative to when the baseline MRI was performed. Sample sizes for the treatment groups are shown in Figure 1.

Based on longitudinal Analysis of Covariance with categorical factors of geographic region, treatment, sex, apolipoprotein E4 genotype, baseline use of vitamin E, baseline Alzheimer's disease medication, study cohort from the initial 78-week trial, and the interaction of time by treatment, with baseline value, the interaction of baseline value and time, the baseline value of Mini Mental State Examination and the baseline value of age included as continuous covariates.

Table 3: Week 78 minus Week 13 percent change from baseline treatment difference versus placebo, model-based least-squares mean (95% CI)

MRI Measure	Verubecestat 12mg - placebo	Verubecestat 40mg - placebo
Total hippocampal volume	0.1 (-0.2, 0.4)	0.0 (-0.3, 0.3)
Left hippocampal volume	0.0 (-0.4, 0.3)	-0.1 (-0.5, 0.3)
Right hippocampal volume	0.2 (-0.1, 0.6)	0.1 (-0.3, 0.5)
Whole brain volume	0.0 (-0.2, 0.1)	0.0 (-0.2, 0.1)
Ventricular volume	-0.8 (-1.8, 0.2)	-0.4 (-1.5, 0.6)
Mayo Cortical Thickness Index	-0.1 (-0.5, 0.2)	0.1 (-0.3, 0.4)

This table shows the difference between the Week 78 and Week 13 values in columns 6 and 8 of Table 2.

Based on longitudinal Analysis of Covariance with categorical factors of geographic region, treatment, sex, apolipoprotein E ϵ 4 genotype, baseline use of vitamin E, baseline Alzheimer's disease medication, study cohort from the initial 78-week trial, and the interaction of time by treatment, with baseline Mayo Cortical Thickness Index, the interaction of baseline Mayo Cortical Thickness Index and time, the baseline value of Mini Mental State Examination and the baseline value of age included as continuous covariates.

Table 4: Cerebrospinal fluid biomarkers of neural injury

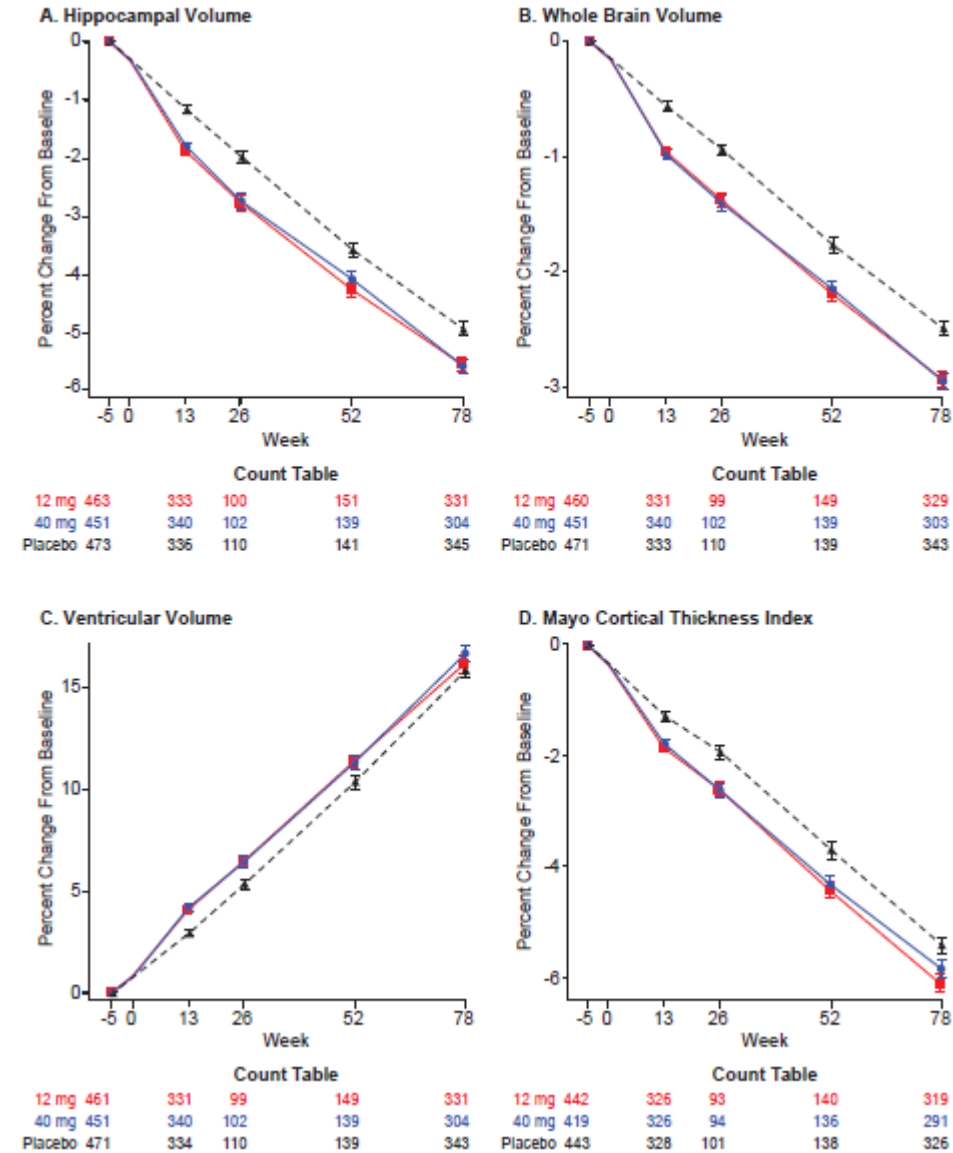
Biomarker	Observed Mean (SD) [n]		Model-based Percent Change from Baseline		
	Baseline	Week 78	LS Mean (95% CI)	Difference vs placebo (95% CI)	p-value
Neurofilament light chain (pg/ml)					
Placebo	1509 (744) [37]	1875 (1416) [37]	19.4 (9.2,29.6)		
Verubecestat 12mg	1529 (621) [31]	1598(615) [31]	7.2 (-3.7,18.1)	-12.2 (-26.7, 2.2)	0.096
Verubecestat 40mg	1723 (644) [50]	1937 (801) [50]	14.6 (5.6,23.5)	-4.8 (-18.0, 8.4)	0.469
Total-Tau (pg/ml)					
Placebo	265.4(351) [37]	284.0 (189) [37]	60.2 (-13.8,134.2)		
Verubecestat 12mg	249.5 (151) [31]	246.1 (123) [31]	-14.1 (-93.2,65.0)	-74.3 (-179,30.6)	0.163
Verubecestat 40mg	318.7 (229) [50]	310.7 (221) [50]	16.2 (-48.0,80.3)	-44.0 (-138,50.1)	0.356
UCHL1 (pg/ml)					
Placebo	2206 (721) [37]	2556 (975) [37]	12.8 (2.1,23.6)		
Verubecestat 12mg	2276 (726) [31]	2477(578) [31]	9.7 (-1.9,21.2)	-3.2 (-18.4,12.1)	0.681
Verubecestat 40mg	2768 (864) [50]	2900 (839) [50]	12.9 (2.9,22.9)	0.0 (-14.3,14.4)	0.999
GFAP (pg/ml)					
Placebo	32071(12690) [37]	33894 (14457) [37]	6.9 (-5.1,18.9)		
Verubecestat 12mg	33758 (14453) [31]	35760 (16843) [31]	6.6 (-6.2,19.4)	-0.3 (-17.3,16.7)	0.973
Verubecestat 40mg	37401 (16439) [50]	42850 (16746) [50]	19.2 (8.6,29.7)	12.3 (-3.2,27.8)	0.119

[†]Based on longitudinal Analysis of Covariance with categorical factors of treatment, sex, apolipoprotein E e4 genotype, and study cohort from the initial 78-week trial with baseline value of the biomarker, the baseline value of Mini Mental State Examination and the baseline value of age included as continuous covariates.

n=Number of subjects with an assessment at that timepoint.

SD=Standard Deviation; LS Mean=Least Squares Mean; CI=Confidence Interval.

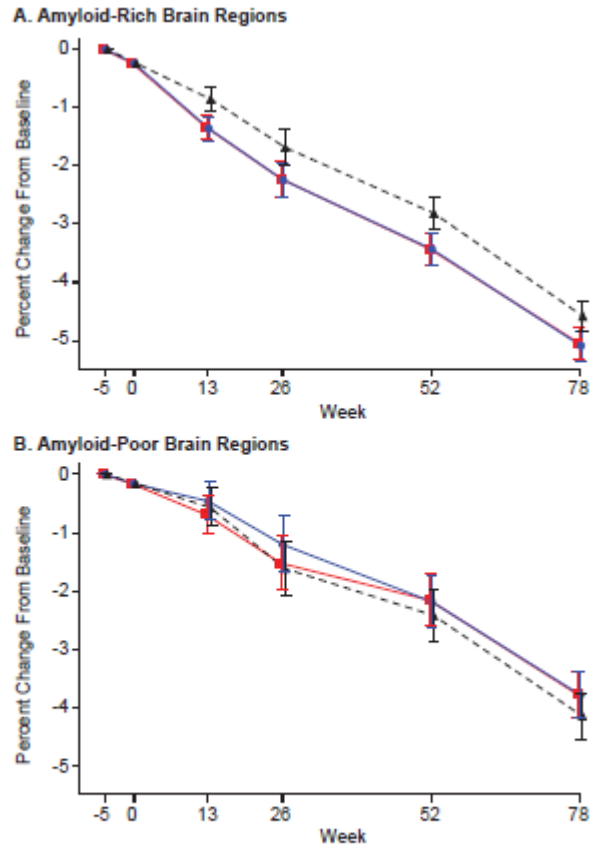
Figure 1. Percent change from baseline (model-based least squares mean \pm standard error) for prespecified brain vMRI measures of A) Hippocampal volume[†], B) Whole brain volume, C) Ventricular volume) and D) Mayo Cortical Thickness Index



Red = verubecestat 12 mg, blue = verubecestat 40 mg, black = placebo.

[†]Left and right hippocampal volume were also prespecified but results are not shown as they were identical to total hippocampal volume.

Figure 2. Percent change from baseline (model-based least squares mean \pm standard error) for vMRI in A) pooled amyloid-rich brain regions, and B) pooled amyloid-poor brain regions (grey and white matter)



Count Table

12 mg	442	327	93	139	319
40 mg	419	326	94	136	291
Placebo	443	329	101	138	326

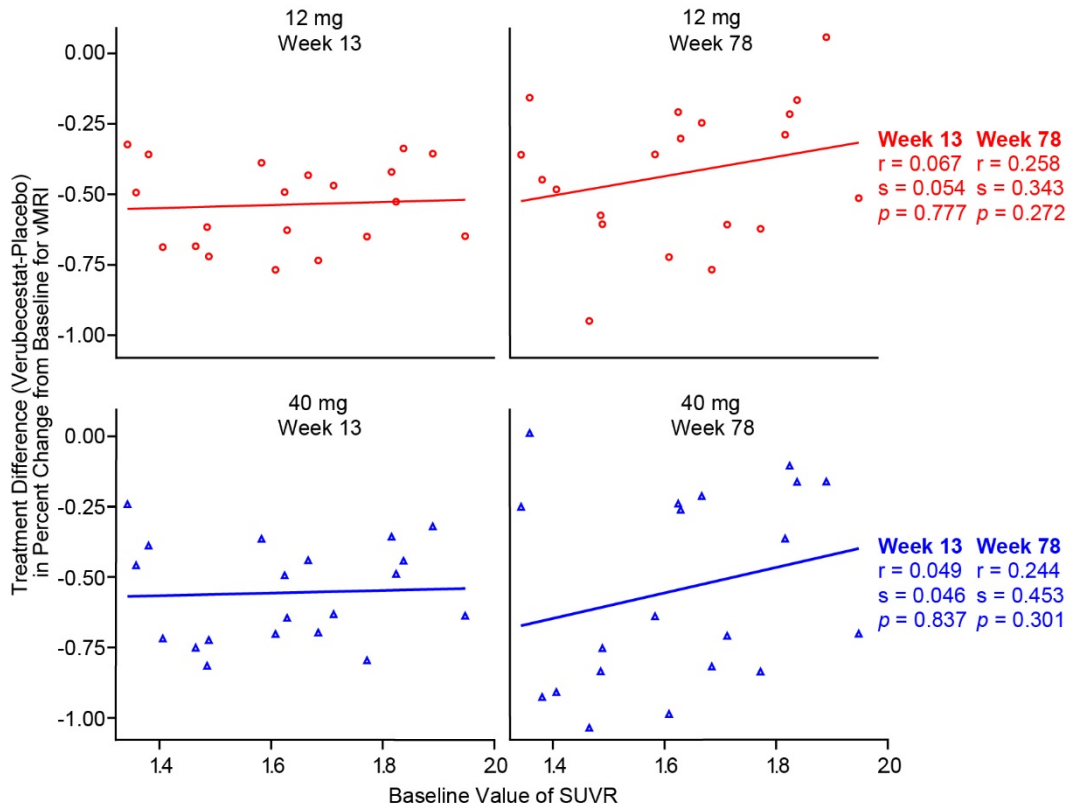
Red = verubecestat 12 mg, blue = verubecestat 40 mg, black = placebo

Amyloid-rich regions: pericalcarine cortex, insula cortex, precentral cortex, amygdala, isthmus cingulate cortex, precuneus cortex, postcentral cortex, lateral occipital cortex, supramarginal cortex, cuneus cortex, lateral orbitofrontal cortex, posterior cingulate cortex, parahippocampal cortex, lingual cortex, paracentral cortex, thalamus, medial orbitofrontal cortex, fusiform cortex, frontal pole cortex, middle temporal cortex, and entorhinal cortex.

Amyloid-poor regions: cerebellum (cortex and white matter), corpus callosum (mid anterior, posterior, central, mid posterior, anterior), and pallidum.

Accepted Version

Figure 3. Scatter plot of baseline value of PET amyloid standardised uptake value ratio versus treatment difference (verubecestat-placebo) in percent change from baseline in vMRI for 20 selected amyloid-rich brain regions with corresponding regression lines[†]



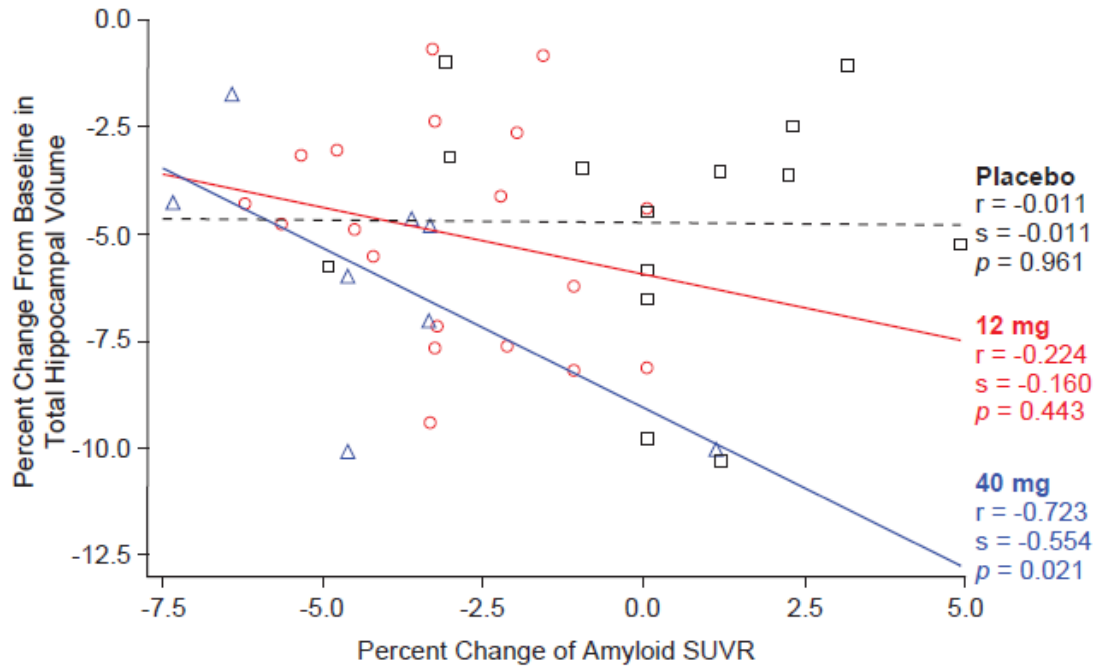
[†]Brain regions were selected to represent the largest possible range of standardised uptake value ratio values at baseline among the regions provided by the Freesurfer segmentation software that automatically define the boundaries of various brain regions on an MRI scan. Each point on the plots represents 1 of the 20 brain regions: pericalcarine cortex, insula cortex, precentral cortex, amygdala, isthmus cingulate cortex, precuneus cortex, postcentral cortex, lateral occipital cortex, supramarginal cortex, cuneus cortex, lateral orbitofrontal cortex, posterior cingulate cortex, parahippocampal cortex, lingual cortex, paracentral cortex, thalamus, medial orbitofrontal cortex, fusiform cortex, frontal pole cortex, middle temporal cortex. Entorhinal cortex (an additional amyloid-rich region) was excluded from this analysis because amyloid PET standardised uptake value ratio for this region was low and not consistent with the known high amyloid deposition in this structure. The numbers of patients contributing to the estimates of baseline standardised uptake value ratio for a brain region are approximately similar to those shown in Table 1. The numbers of patients contributing to the estimates of vMRI for a brain region are approximately similar to those shown in Figure 2.

r = observed Pearson correlation coefficient
 s = model-based slope estimate for regression line
 p = p-value for slope estimate

Red = verubecestat 12 mg-placebo, blue = verubecestat 40 mg-placebo.

Accepted Version

Figure 4. Scatter plot of percent change from baseline in MRI total hippocampal volume at Week 78 versus percent change from baseline in amyloid PET standardised uptake value ratio at Week 78[†]



[†]Each point on this plot is an individual patient (placebo N=14, 12mg N=19, 40mg N=9). There is no equivalent plot for Week 13 because PET data were not gathered at Week 13.

r = observed Pearson correlation coefficient
s = model-based slope estimate for regression line
p = p-value for slope estimate

Red = verubecestat 12 mg, blue = verubecestat 40 mg, black = placebo.

Figure Legends

Figure 1. Percent change from baseline (model-based least squares mean \pm standard error) for prespecified brain vMRI measures of A) Hippocampal volume[†], B) Whole brain volume, C) Ventricular volume) and D) Mayo Cortical Thickness Index

Footnotes

Red = verubecestat 12 mg, blue = verubecestat 40 mg, black = placebo.

[†]Left and right hippocampal volume were also prespecified but results are not shown as they were identical to total hippocampal volume.

Figure 2. Percent change from baseline (model-based least squares mean \pm standard error) for vMRI in A) pooled amyloid-rich brain regions, and B) pooled amyloid-poor brain regions (grey and white matter) Footnotes

Amyloid-rich regions: pericalcarine cortex, insula cortex, precentral cortex, amygdala, isthmus cingulate cortex, precuneus cortex, postcentral cortex, lateral occipital cortex, supramarginal cortex, cuneus cortex, lateral orbitofrontal cortex, posterior cingulate cortex, parahippocampal cortex, lingual cortex, paracentral cortex, thalamus, medial orbitofrontal cortex, fusiform cortex, frontal pole cortex, middle temporal cortex, and entorhinal cortex.

Amyloid-poor regions: cerebellum (cortex and white matter), corpus callosum (mid anterior, posterior, central, mid posterior, anterior), and pallidum.

Figure 3. Scatter plot of baseline value of PET amyloid standardised uptake value ratio versus treatment difference (verubecestat-placebo) in percent change from baseline in vMRI for 20 selected amyloid-rich brain regions with corresponding regression lines[†]

Footnotes

[†]Brain regions were selected to represent the largest possible range of standardised uptake value ratio values at baseline among the regions provided by the Freesurfer segmentation software that automatically define the boundaries of various brain regions on an MRI scan. Each point on the plots represents 1 of the 20 brain regions: pericalcarine cortex, insula cortex, precentral cortex, amygdala, isthmus cingulate cortex, precuneus cortex, postcentral cortex, lateral occipital cortex, supramarginal cortex,

cuneus cortex, lateral orbitofrontal cortex, posterior cingulate cortex, parahippocampal cortex, lingual cortex, paracentral cortex, thalamus, medial orbitofrontal cortex, fusiform cortex, frontal pole cortex, middle temporal cortex. Entorhinal cortex (an additional amyloid-rich region) was excluded from this analysis because amyloid PET standardised uptake value ratio for this region was low and not consistent with the known high amyloid deposition in this structure. The numbers of patients contributing to the estimates of baseline standardised uptake value ratio for a brain region are approximately similar to those shown in Table 1. The numbers of patients contributing to the estimates of vMRI for a brain region are approximately similar to those shown in Figure 2.

r = observed Pearson correlation coefficient
s = model-based slope estimate for regression line
p = p-value for slope estimate

Figure 4. Scatter plot of percent change from baseline in MRI total hippocampal volume at Week 78 versus percent change from baseline in amyloid PET standardised uptake value ratio at Week 78[†]

Footnotes

[†]Each point on this plot is an individual patient (placebo N=14, 12mg N=19, 40mg N=9). There is no equivalent plot for Week 13 because PET data were not gathered at Week 13.

r = observed Pearson correlation coefficient
s = model-based slope estimate for regression line
p = p-value for slope estimate

Red = verubecestat 12 mg, blue = verubecestat 40 mg, black = placebo.

Supplementary data

Accepted Version

Supplementary Table S1. Subgroup analyses of percent change from baseline in MRI total hippocampal volume at Week 13 and Week 78, model-based least-squares mean (standard error) and difference (95% CI) versus placebo

Timepoint and subgroup	Mean (SE) Change [n]			Difference (95% CI)	
	Verubecestat 12mg	Verubecestat 40mg	Placebo	12mg vs placebo	40mg vs placebo
Week 13					
<i>Mini Mental State Examination severity</i>					
Mild (≥ 21)	-1.9 (0.1) [160]	-1.8 (0.1) [163]	-1.2 (0.1) [165]	-0.7 (-1.0, -0.4)	-0.6 (-0.9, -0.3)
Moderate (≤ 20)	-1.9 (0.1) [173]	-1.8 (0.1) [178]	-1.2 (0.1) [173]	-0.7 (-1.0, -0.4)	-0.6 (-0.9, -0.3)
<i>Apolipoprotein E e4 genotype</i>					
Non-carrier	-1.9 (0.1) [117]	-1.5 (0.1) [127]	-1.2 (0.1) [105]	-0.7 (-1.0, -0.3)	-0.3 (-0.6, 0.1)
Carrier	-1.9 (0.1) [216]	-2.0 (0.1) [215]	-1.2 (0.1) [233]	-0.7 (-1.0, -0.5)	-0.8 (-1.1, -0.6)
<i>Age</i>					
< 73 years	-1.7 (0.1) [182]	-1.8 (0.1) [179]	-1.2 (0.1) [168]	-0.6 (-0.9, -0.3)	-0.6 (-1.0, -0.3)
≥ 73 years	-2.1 (0.1) [151]	-1.8 (0.1) [164]	-1.2 (0.1) [172]	-0.8 (-1.1, -0.6)	-0.6 (-0.9, -0.3)
<i>Sex</i>					
Men	-1.9 (0.1) [150]	-1.8 (0.1) [146]	-1.2 (0.1) [163]	-0.7 (-1.0, -0.4)	-0.6 (-0.9, -0.3)
Women	-1.8 (0.1) [183]	-1.8 (0.1) [197]	-1.2 (0.1) [177]	-0.7 (-1.0, -0.4)	-0.6 (-0.9, -0.3)
Week 78					
<i>Mini Mental State Examination severity</i>					
Mild (≥ 21)	-5.6 (0.2) [169]	-5.8 (0.2) [153]	-4.9 (0.2) [165]	-0.7 (-1.1, -0.3)	-0.9 (-1.3, -0.4)
Moderate (≤ 20)	-5.7 (0.2) [162]	-5.4 (0.2) [153]	-5.1 (0.2) [180]	-0.6 (-1.1, -0.1)	-0.4 (-0.9, 0.1)
<i>Apolipoprotein E e4 genotype</i>					
Carrier	-5.7 (0.2) [118]	-5.1 (0.2) [109]	-4.8 (0.2) [116]	-0.9 (-1.4, -0.3)	-0.3 (-0.8, 0.3)
Noncarrier	-5.5 (0.1) [214]	-5.9 (0.1) [197]	-5.1 (0.1) [231]	-0.4 (-0.9, 0.0)	-0.8 (-1.2, -0.4)
<i>Age</i>					
< 73 years	-5.5 (0.2) [190]	-5.8 (0.1) [172]	-5.0 (0.2) [181]	-0.5 (-0.9, 0.0)	-0.8 (-1.2, -0.3)
≥ 73 years	-5.7 (0.2) [142]	-5.5 (0.2) [136]	-5.0 (0.2) [166]	-0.7 (-1.2, -0.3)	-0.5 (-1.0, 0.0)

Sex					
Men	-5.9 (0.2) [146]	-5.7 (0.2) [122]	-5.0 (0.2) [153]	-0.9 (-1.3, -0.4)	-0.7 (-1.2, -0.2)
Women	-5.3 (0.2) [186]	-5.5 (0.2) [186]	-4.9 (0.2) [194]	-0.4 (-0.8, 0.0)	-0.6 (-1.0, -0.2)

Accepted Version

Supplementary Table S2: Percent change in MRI volume from baseline to Week 13 and Week 78 for selected brain regions, model-based

least-squares mean (95% CI) and difference (95% CI) versus placebo

Brain Region	Timepoint ^a	Mean Change from Baseline ^a (95% CI)			Difference vs Placebo (95% CI) [p-value]	
		Verubecestat 12 mg	Verubecestat 40 mg	Placebo	12 mg vs placebo	40 mg vs placebo
Amygdala	Week 13	-1.6 (-1.8, -1.4)	-1.5 (-1.8, -1.3)	-1.1 (-1.3, -0.9)	-0.5 (-0.8, -0.2) [0.001]	-0.4 (-0.7, -0.1) [0.010]
	Week 78	-5.7 (-6.0, -5.4)	-5.3 (-5.6, -5.0)	-5.4 (-5.7, -5.1)	-0.3 (-0.7, 0.1) [0.189]	0.1 (-0.4, 0.5) [0.732]
Caudate	Week 13	-0.4 (-0.5, -0.2)	-0.3 (-0.4, -0.1)	-0.3 (-0.4, -0.2)	-0.1 (-0.3, 0.1) [0.591]	0.0 (-0.2, 0.2) [0.774]
	Week 78	-0.3 (-0.5, -0.1)	0.1 (-0.1, 0.4)	-0.6 (-0.8, -0.4)	0.3 (0.0, 0.6) [0.040]	0.8 (0.4, 1.1) [$<.001$]
Corpus Callosum Central	Week 13	-1.1 (-1.4, -0.7)	-0.9 (-1.3, -0.4)	-1.0 (-1.4, -0.6)	-0.1 (-0.6, 0.5) [0.830]	0.1 (-0.5, 0.7) [0.680]
	Week 78	-1.3 (-1.7, -0.9)	-1.4 (-1.8, -1.0)	-2.2 (-2.5, -1.8)	0.9 (0.4, 1.5) [0.001]	0.8 (0.2, 1.3) [0.007]
Corpus Callosum Anterior	Week 13	-1.4 (-1.8, -1.1)	-1.2 (-1.6, -0.9)	-1.0 (-1.4, -0.7)	-0.4 (-0.9, 0.1) [0.110]	-0.2 (-0.7, 0.3) [0.432]
	Week 78	-2.8 (-3.1, -2.4)	-2.8 (-3.2, -2.4)	-3.3 (-3.6, -2.9)	0.5 (-0.0, 1.0) [0.051]	0.5 (-0.0, 1.0) [0.066]
Corpus Callosum Mid Posterior	Week 13	-1.1 (-1.5, -0.7)	-1.0 (-1.4, -0.6)	-1.0 (-1.4, -0.6)	-0.1 (-0.7, 0.4) [0.683]	-0.0 (-0.6, 0.5) [0.950]
	Week 78	-2.4 (-2.8, -2.0)	-2.4 (-2.9, -2.0)	-3.1 (-3.5, -2.6)	0.7 (0.1, 1.3) [0.020]	0.6 (0.0, 1.3) [0.039]
Corpus Callosum Posterior	Week 13	-1.1 (-1.3, -0.8)	-0.9 (-1.2, -0.7)	-1.1 (-1.3, -0.8)	0.0 (-0.4, 0.4) [0.997]	0.1 (-0.2, 0.5) [0.488]
	Week 78	-4.3 (-4.6, -4.0)	-4.3 (-4.7, -3.9)	-4.3 (-4.6, -4.0)	0.0 (-0.5, 0.5) [0.988]	0.0 (-0.5, 0.5) [0.991]
Corpus Callosum Mid Anterior	Week 13	-1.6 (-2.1, -1.2)	-1.1 (-1.6, -0.7)	-1.4 (-1.8, -0.9)	-0.3 (-0.9, 0.4) [0.403]	0.2 (-0.4, 0.9) [0.465]
	Week 78	-2.5 (-3.0, -2.0)	-2.7 (-3.1, -2.2)	-3.3 (-3.7, -2.9)	0.8 (0.2, 1.4) [0.012]	0.6 (0.0, 1.2) [0.046]
Cerebellum Cortex	Week 13	-0.3 (-0.4, -0.2)	-0.1 (-0.2, -0.0)	-0.3 (-0.3, -0.2)	-0.0 (-0.1, 0.1) [0.758]	0.2 (0.1, 0.3) [0.005]
	Week 78	-0.9 (-1.0, -0.8)	-0.8 (-1.0, -0.7)	-1.0 (-1.1, -0.8)	0.0 (-0.1, 0.2) [0.708]	0.1 (-0.0, 0.3) [0.154]
Cerebellum White Matter	Week 13	-0.4 (-0.6, -0.3)	-0.4 (-0.5, -0.2)	-0.2 (-0.4, -0.1)	-0.2 (-0.4, -0.0) [0.042]	-0.1 (-0.3, 0.1) [0.279]
	Week 78	-1.6 (-1.8, -1.5)	-1.6 (-1.8, -1.4)	-1.5 (-1.6, -1.3)	-0.2 (-0.4, 0.1) [0.169]	-0.1 (-0.3, 0.1) [0.342]
Cuneus Cortex	Week 13	-1.3 (-1.4, -1.1)	-1.3 (-1.5, -1.1)	-0.6 (-0.8, -0.4)	-0.7 (-0.9, -0.4) [$<.001$]	-0.7 (-1.0, -0.4) [$<.001$]
	Week 78	-2.5 (-2.8, -2.3)	-2.9 (-3.1, -2.7)	-2.0 (-2.2, -1.7)	-0.5 (-0.9, -0.2) [0.002]	-0.9 (-1.3, -0.6) [$<.001$]
Entorhinal Cortex	Week 13	-1.9 (-2.1, -1.7)	-1.5 (-1.7, -1.3)	-1.6 (-1.8, -1.3)	-0.4 (-0.7, -0.0) [0.029]	0.0 (-0.3, 0.3) [0.803]
	Week 78	-6.8 (-7.1, -6.4)	-6.2 (-6.5, -5.8)	-6.5 (-6.8, -6.2)	-0.3 (-0.8, 0.2) [0.209]	0.3 (-0.2, 0.8) [0.201]
Frontal Pole Cortex	Week 13	-1.3 (-1.6, -1.0)	-1.3 (-1.6, -1.0)	-0.8 (-1.1, -0.5)	-0.5 (-0.9, -0.1) [0.022]	-0.5 (-1.0, -0.1) [0.017]
	Week 78	-2.8 (-3.2, -2.5)	-2.8 (-3.2, -2.4)	-2.5 (-2.8, -2.2)	-0.3 (-0.8, 0.2) [0.197]	-0.3 (-0.8, 0.2) [0.238]
Fusiform Cortex	Week 13	-2.1 (-2.2, -1.9)	-2.0 (-2.2, -1.9)	-1.3 (-1.5, -1.2)	-0.7 (-0.9, -0.5) [$<.001$]	-0.7 (-0.9, -0.5) [$<.001$]

Insula Cortex	Week 78	-6.4 (-6.6, -6.1)	-6.4 (-6.7, -6.1)	-5.5 (-5.7, -5.2)	-0.9 (-1.3, -0.5) [$<.001$]	-1.0 (-1.4, -0.6) [$<.001$]
	Week 13	-1.9 (-2.0, -1.7)	-1.9 (-2.1, -1.8)	-1.3 (-1.4, -1.1)	-0.6 (-0.8, -0.4) [$<.001$]	-0.7 (-0.9, -0.5) [$<.001$]
Isthmus Cingulate Cortex	Week 78	-4.8 (-5.0, -4.6)	-4.7 (-4.9, -4.4)	-4.4 (-4.6, -4.2)	-0.4 (-0.7, -0.1) [0.011]	-0.3 (-0.6, 0.0) [0.080]
	Week 13	-1.6 (-1.8, -1.4)	-1.6 (-1.8, -1.4)	-1.2 (-1.4, -1.0)	-0.4 (-0.6, -0.1) [0.002]	-0.4 (-0.6, -0.1) [0.002]
Lateral Occipital Cortex	Week 78	-4.4 (-4.6, -4.1)	-4.4 (-4.6, -4.1)	-4.1 (-4.3, -3.8)	-0.3 (-0.6, 0.0) [0.087]	-0.3 (-0.7, 0.0) [0.075]
	Week 13	-1.2 (-1.3, -1.0)	-1.4 (-1.5, -1.2)	-0.6 (-0.7, -0.4)	-0.6 (-0.8, -0.4) [$<.001$]	-0.8 (-1.0, -0.6) [$<.001$]
Lateral Orbitofrontal Cortex	Week 78	-2.5 (-2.6, -2.3)	-2.7 (-2.9, -2.5)	-1.8 (-2.0, -1.6)	-0.6 (-0.9, -0.3) [$<.001$]	-0.9 (-1.2, -0.6) [$<.001$]
	Week 13	-1.4 (-1.6, -1.3)	-1.4 (-1.6, -1.3)	-1.0 (-1.1, -0.8)	-0.5 (-0.7, -0.3) [$<.001$]	-0.5 (-0.7, -0.3) [$<.001$]
Lingual Cortex	Week 78	-3.8 (-4.1, -3.6)	-3.7 (-3.9, -3.4)	-3.6 (-3.8, -3.3)	-0.3 (-0.6, 0.0) [0.095]	-0.1 (-0.4, 0.2) [0.480]
	Week 13	-1.2 (-1.3, -1.0)	-1.2 (-1.4, -1.0)	-0.8 (-1.0, -0.6)	-0.4 (-0.6, -0.1) [0.003]	-0.4 (-0.7, -0.2) [0.001]
Medial Orbitofrontal Cortex	Week 78	-2.8 (-3.0, -2.5)	-3.2 (-3.4, -2.9)	-2.2 (-2.5, -2.0)	-0.5 (-0.8, -0.2) [$<.001$]	-0.9 (-1.2, -0.6) [$<.001$]
	Week 13	-1.3 (-1.5, -1.1)	-1.4 (-1.6, -1.2)	-1.0 (-1.2, -0.7)	-0.4 (-0.7, -0.1) [0.012]	-0.4 (-0.7, -0.2) [0.002]
Middle Temporal Cortex	Week 78	-3.1 (-3.4, -2.9)	-3.1 (-3.3, -2.8)	-2.9 (-3.1, -2.7)	-0.3 (-0.6, 0.1) [0.140]	-0.2 (-0.5, 0.1) [0.265]
	Week 13	-1.5 (-1.6, -1.4)	-1.6 (-1.7, -1.4)	-1.1 (-1.3, -1.0)	-0.4 (-0.5, -0.2) [$<.001$]	-0.4 (-0.6, -0.3) [$<.001$]
Pallidum	Week 78	-5.1 (-5.3, -4.9)	-4.9 (-5.1, -4.7)	-4.7 (-4.9, -4.4)	-0.4 (-0.7, -0.1) [0.010]	-0.2 (-0.6, 0.1) [0.152]
	Week 13	-0.5 (-0.7, -0.4)	-0.3 (-0.4, -0.2)	-0.5 (-0.6, -0.3)	-0.1 (-0.3, 0.1) [0.472]	0.2 (-0.0, 0.4) [0.082]
Parahippocampal Cortex	Week 78	-1.7 (-1.8, -1.5)	-1.5 (-1.7, -1.4)	-1.7 (-1.9, -1.5)	0.0 (-0.2, 0.3) [0.782]	0.2 (-0.1, 0.4) [0.236]
	Week 13	-1.9 (-2.1, -1.7)	-1.9 (-2.1, -1.6)	-1.6 (-1.8, -1.4)	-0.3 (-0.6, -0.0) [0.036]	-0.2 (-0.5, 0.0) [0.090]
Paracentral Cortex	Week 78	-6.0 (-6.3, -5.7)	-5.8 (-6.2, -5.5)	-5.6 (-5.9, -5.4)	-0.4 (-0.8, 0.0) [0.053]	-0.2 (-0.6, 0.2) [0.342]
	Week 13	-1.4 (-1.6, -1.2)	-1.6 (-1.8, -1.4)	-1.0 (-1.2, -0.8)	-0.4 (-0.7, -0.1) [0.006]	-0.6 (-0.9, -0.3) [$<.001$]
Pericalcarine Cortex	Week 78	-3.1 (-3.4, -2.9)	-3.2 (-3.4, -3.0)	-2.5 (-2.7, -2.2)	-0.6 (-1.0, -0.3) [$<.001$]	-0.7 (-1.0, -0.4) [$<.001$]
	Week 13	-1.1 (-1.3, -0.9)	-1.0 (-1.2, -0.8)	-0.7 (-0.9, -0.5)	-0.4 (-0.7, -0.2) [0.003]	-0.4 (-0.6, -0.1) [0.008]
Posterior Cingulate Cortex	Week 78	-1.7 (-1.9, -1.5)	-1.9 (-2.2, -1.7)	-1.3 (-1.5, -1.0)	-0.4 (-0.8, -0.1) [0.014]	-0.6 (-1.0, -0.3) [$<.001$]
	Week 13	-1.5 (-1.7, -1.3)	-1.6 (-1.7, -1.4)	-1.2 (-1.4, -1.0)	-0.3 (-0.5, -0.0) [0.038]	-0.3 (-0.6, -0.1) [0.012]
Postcentral Cortex	Week 78	-4.0 (-4.2, -3.7)	-4.2 (-4.4, -3.9)	-4.0 (-4.3, -3.7)	0.0 (-0.3, 0.4) [0.894]	-0.2 (-0.6, 0.2) [0.410]
	Week 13	-1.2 (-1.4, -1.1)	-1.3 (-1.5, -1.2)	-0.6 (-0.7, -0.4)	-0.7 (-0.9, -0.5) [$<.001$]	-0.8 (-1.0, -0.6) [$<.001$]
Precuneus Cortex	Week 78	-2.4 (-2.6, -2.3)	-2.5 (-2.7, -2.4)	-1.5 (-1.6, -1.3)	-1.0 (-1.2, -0.7) [$<.001$]	-1.0 (-1.2, -0.8) [$<.001$]
	Week 13	-1.9 (-2.0, -1.7)	-1.9 (-2.1, -1.7)	-1.3 (-1.5, -1.1)	-0.6 (-0.8, -0.3) [$<.001$]	-0.6 (-0.9, -0.4) [$<.001$]
Precentral Cortex	Week 78	-5.3 (-5.5, -5.0)	-5.4 (-5.7, -5.1)	-4.7 (-5.0, -4.4)	-0.6 (-1.0, -0.2) [0.003]	-0.7 (-1.1, -0.3) [$<.001$]
	Week 13	-1.6 (-1.7, -1.5)	-1.6 (-1.8, -1.5)	-0.9 (-1.1, -0.8)	-0.7 (-0.9, -0.5) [$<.001$]	-0.7 (-0.9, -0.5) [$<.001$]

Putamen	Week 78	-3.2 (-3.4, -3.0)	-3.3 (-3.5, -3.2)	-2.6 (-2.8, -2.4)	-0.6 (-0.8, -0.3) [$<.001$]	-0.8 (-1.0, -0.5) [$<.001$]
	Week 13	-0.6 (-0.7, -0.5)	-0.4 (-0.5, -0.3)	-0.6 (-0.7, -0.5)	-0.0 (-0.2, 0.2) [0.980]	0.2 (0.0, 0.4) [0.014]
Supramarginal Cortex	Week 78	-2.3 (-2.5, -2.1)	-2.0 (-2.2, -1.8)	-2.4 (-2.6, -2.2)	0.1 (-0.2, 0.3) [0.546]	0.4 (0.1, 0.7) [0.003]
	Week 13	-1.7 (-1.8, -1.5)	-1.7 (-1.8, -1.5)	-1.0 (-1.1, -0.8)	-0.7 (-0.9, -0.5) [$<.001$]	-0.7 (-0.9, -0.5) [$<.001$]
Thalamus	Week 78	-4.4 (-4.6, -4.2)	-4.4 (-4.6, -4.2)	-3.6 (-3.8, -3.4)	-0.8 (-1.1, -0.5) [$<.001$]	-0.8 (-1.1, -0.5) [$<.001$]
	Week 13	-1.2 (-1.3, -1.1)	-1.4 (-1.5, -1.3)	-0.6 (-0.7, -0.5)	-0.6 (-0.8, -0.5) [$<.001$]	-0.8 (-0.9, -0.7) [$<.001$]
	Week 78	-3.5 (-3.7, -3.4)	-3.8 (-4.0, -3.6)	-2.9 (-3.1, -2.7)	-0.6 (-0.9, -0.4) [$<.001$]	-0.9 (-1.1, -0.7) [$<.001$]

^a Note: baseline MRI was performed a mean of -5 weeks prior to the initiation of treatment. The timepoints shown (Week 13 and Week 78) are relative to the initiation of treatment, not relative to when the baseline MRI was performed. Sample sizes for the treatment groups are shown in Figure 2.

Based on longitudinal Analysis of Covariance with categorical factors of geographic region, treatment, sex, apolipoprotein E $\epsilon 4$ genotype, baseline use of vitamin E, baseline Alzheimer's disease medication, study cohort from the initial 78-week trial, and the interaction of time by treatment, with baseline value, the interaction of baseline value and time, the baseline value of Mini Mental State Examination and the baseline value of age included as continuous covariates.

Supplementary Table S3. Model-based analyses[†] of percent change from baseline at Week 13 (with 95% CI and p-value) in vMRI brain regions categorized by amyloid load or timing of amyloid deposition

	% Change (95% CI) [p-value]			Treatment difference (95% CI) [p-value]	
	Verubecestat 12mg	Verubecestat 40mg	Placebo	Verubecestat 12mg - Placebo	Verubecestat 40mg - Placebo
<i>Categorized by amyloid load</i>					
Amyloid-rich regions	-1.34 (-1.74, -0.94) [<0.001]	-1.36 (-1.76, -0.95) [<0.001]	-0.85 (-1.26, -0.45) [<0.001]	-0.49 (-0.63, -0.35) [<0.001]	-0.50 (-0.66, -0.35) [<0.001]
Amyloid-poor regions	-0.69 (-1.32, -0.07) [0.029]	-0.46 (-1.08, 0.16) [0.143]	-0.57 (-1.18, 0.05) [0.070]	-0.13 (-0.36, 0.11) [0.286]	0.11 (-0.13, 0.34) [0.374]
<i>Categorized by timing of amyloid deposition</i>					
Early amyloid deposition regions	-1.64 (-1.79, -1.49) [<0.001]	-1.67 (-1.83, -1.52) [<0.001]	-1.21 (-1.36, -1.06) [<0.001]	-0.43 (-0.60, -0.25) [<0.001]	-0.46 (-0.64, -0.29) [<0.001]
Late amyloid deposition regions	-1.34 (-1.50, -1.17) [<0.001]	-1.39 (-1.56, -1.23) [<0.001]	-0.84 (-1.01, -0.68) [<0.001]	-0.49 (-0.67, -0.31) [<0.001]	-0.55 (-0.73, -0.37) [<0.001]
No amyloid regions	-0.57 (-1.00, -0.13) [0.011]	-0.35 (-0.78, 0.08) [0.113]	-0.54 (-0.97, -0.10) [0.015]	-0.03 (-0.16, 0.09) [0.632]	0.19 (0.06, 0.31) [0.003]

[†]Analysis of covariance model with categorical terms for treatment, amyloid category (Amyloid-rich, Amyloid-poor or Early amyloid deposition, Late amyloid deposition, No amyloid), and week, along with all two-way and three-way interactions, also including terms for baseline and the interaction of baseline and week. The dependent variable is the average percent change from baseline of all brain regions in the given amyloid category at the given week. Sample sizes for the treatment groups are shown in Figure 2 and Figure S1.

Amyloid-rich regions: Pericalcarine cortex, insula cortex, precentral cortex, amygdala, isthmus cingulate cortex, precuneus cortex, postcentral cortex, lateral occipital cortex, supramarginal cortex, cuneus cortex, lateral orbitofrontal cortex, posterior cingulate cortex, parahippocampal cortex, lingual cortex, paracentral cortex, thalamus, medial orbitofrontal cortex, fusiform cortex, frontal pole cortex, middle temporal cortex, entorhinal cortex.

Amyloid-poor regions: Cerebellum (cortex and white matter), corpus callosum (mid anterior, posterior, central, mid posterior, anterior), pallidum.

Early amyloid deposition regions: Precuneus, posterior cingulate, isthmus cingulate, insula, and medial and lateral orbitofrontal cortices.

Late amyloid deposition regions: Lingual, pericalcarine, paracentral, precentral, and postcentral cortices.

No amyloid regions: Cerebellar cortex, pallidum.

Supplementary Table S4. Model-based slopes for regression[†] of ADAS-Cog₁₁ total score on vMRI parameters at Week 13 and

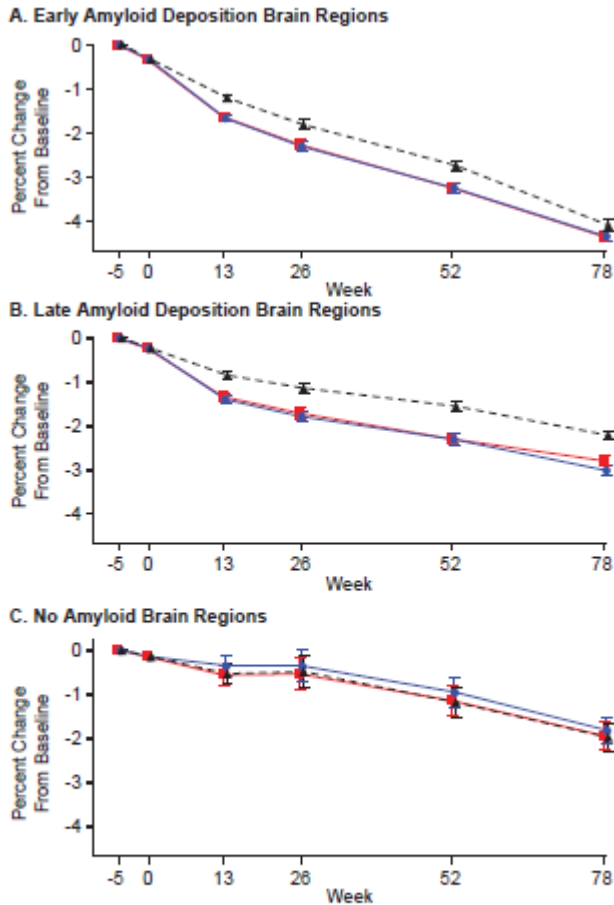
Week 78

	Verubecestat 12mg				Verubecestat 40mg				Placebo			
	n	Observed Pearson Correlation	Slope Estimate (95% CI)	p-value	n	Observed Pearson Correlation	Slope Estimate (95% CI)	p-value	n	Observed Pearson Correlation	Slope Estimate (95% CI)	p-value
Week 13												
Total Hippocampal												
Volume	332	-0.137	-0.413 (-0.750, -0.077)	0.016	338	0.052	0.164 (-0.164, 0.491)	0.327	339	0.004	0.014 (-0.345, 0.374)	0.937
Left Hippocampal												
Volume	332	-0.152	-0.401 (-0.695, -0.107)	0.008	338	0.053	0.138 (-0.132, 0.408)	0.315	339	-0.021	-0.061 (-0.372, 0.250)	0.702
Right Hippocampal												
Volume	332	-0.078	-0.201 (-0.489, 0.087)	0.172	338	0.032	0.093 (-0.210, 0.397)	0.547	339	0.030	0.084 (-0.219, 0.387)	0.587
Whole Brain												
Volume	330	-0.146	-0.928 (-1.636, -0.220)	0.010	338	-0.113	-0.695 (-1.329, -0.062)	0.032	336	-0.046	-0.281 (-0.945, 0.383)	0.406
Ventricular												
Volume	330	0.124	0.175 (0.018, 0.333)	0.029	338	0.095	0.150 (-0.013, 0.312)	0.071	337	0.008	0.013 (-0.165, 0.190)	0.889
Mayo Cortical Thickness												
Index	326	-0.103	-0.361 (-0.760, 0.038)	0.076	325	-0.075	-0.292 (-0.697, 0.114)	0.158	331	0.014	0.055 (-0.370, 0.479)	0.801
Week 78												
Total Hippocampal												
Volume	310	0.038	0.111 (-0.218, 0.440)	0.508	292	-0.087	-0.268 (-0.635, 0.099)	0.153	338	-0.089	-0.286 (-0.615, 0.044)	0.089
Left Hippocampal												
Volume	310	0.010	0.027 (-0.267, 0.321)	0.858	292	-0.100	-0.278 (-0.611, 0.055)	0.102	338	-0.073	-0.203 (-0.490, 0.084)	0.165
Right Hippocampal												
Volume	310	0.062	0.168 (-0.138, 0.473)	0.281	292	-0.062	-0.172 (-0.505, 0.160)	0.310	338	-0.093	-0.283 (-0.596, 0.030)	0.077
Whole Brain												
Volume	308	-0.545	-3.174 (-3.745, -2.603)	<0.001	291	-0.448	-2.492 (-3.065, -1.920)	<0.001	336	-0.517	-3.235 (-3.796, -2.675)	<0.001
Ventricular												
Volume	310	0.474	0.405 (0.320, 0.491)	<0.001	292	0.445	0.381 (0.290, 0.472)	<0.001	336	0.450	0.416 (0.331, 0.502)	<0.001
Mayo Cortical Thickness												
Index	299	-0.442	-1.174 (-1.445, -0.903)	<0.001	282	-0.461	-1.210 (-1.493, -0.927)	<0.001	324	-0.485	-1.503 (-1.793, -1.213)	<0.001

[†]Model regressed ADAS-Cog₁₁ on the given volumetric MRI parameter.

All volumetric MRI units are in microliters, except for Mayo Cortical Thickness Index which is in mm.

Supplementary Figure S1. Percent change from baseline (model-based least squares mean \pm standard error) for vMRI in A) pooled early amyloid deposition brain regions, B) pooled late amyloid deposition brain regions, and C) pooled no amyloid areas



Count Table

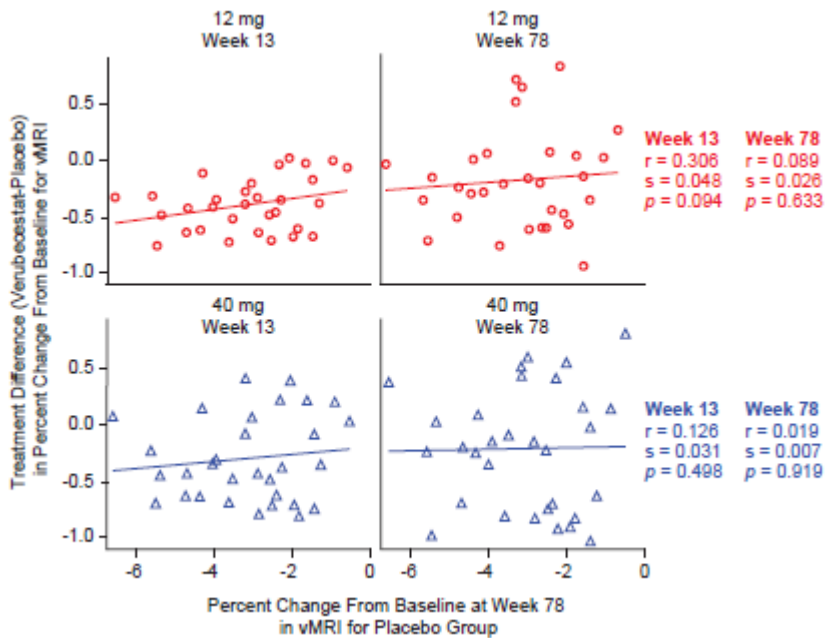
12 mg	442	327	93	139	319
40 mg	419	326	94	136	291
Placebo	443	329	101	138	326

Early amyloid deposition regions: Precuneus, posterior cingulate, isthmus cingulate, insula, and medial and lateral orbitofrontal cortices.

Late amyloid deposition regions: Lingual, pericalcarine, paracentral, precentral, and postcentral cortices.

No amyloid regions: Cerebellar cortex, pallidum.

Supplementary Figure S2. Scatter plot of percent change from baseline at Week 78 in vMRI for the placebo group (i.e., the amount of AD-related neurodegeneration) versus treatment difference (verubecestat-placebo) in percent change from baseline in vMRI for 31 selected brain regions with corresponding regression lines[†]



[†]Brain regions were selected to obtain a large range of AD-related neurodegeneration values among regions provided by the Freesurfer segmentation software that automatically defines the boundaries of various brain regions on an MRI scan. For this analysis, white matter regions as well as amyloid-poor and amyloid-rich regions were included. Each point on the plots represents 1 of the 31 brain regions: pericalcarine cortex, insula cortex, precentral cortex, amygdala, isthmus cingulate cortex, precuneus cortex, postcentral cortex, lateral occipital cortex, supramarginal cortex, cuneus cortex, lateral orbitofrontal cortex, posterior cingulate cortex, parahippocampal cortex, lingual cortex, paracentral cortex, thalamus, medial orbitofrontal cortex, fusiform cortex, frontal pole cortex, middle temporal cortex, caudate, entorhinal cortex, putamen, pallidum, cerebellum white matter, cerebellum cortex, corpus callosum (posterior, mid posterior, mid anterior, central, anterior). The numbers of patients contributing to the vMRI estimates for a brain region are approximately similar to those shown in Figure 2.

r = observed Pearson correlation coefficient
 s = model-based slope estimate for regression line
 p = p-value for slope estimate

Red = verubecestat 12 mg-placebo, blue = verubecestat 40 mg-placebo

Accepted Version